

Lithium Batteries

International Edition: DOI: 10.1002/anie.201907805

German Edition: DOI: 10.1002/ange.201907805

An Illumination-Assisted Flexible Self-Powered Energy System Based on a Li–O₂ Battery

Xiao-yang Yang, Xi-lan Feng, Xin Jin, Ming-zhe Shao, Bao-lin Yan, Jun-min Yan,* Yu Zhang,* and Xin-bo Zhang*

Abstract: The flexible Li–O₂ battery is suitable to satisfy the requirements of a self-powered energy system, thanks to environmental friendliness, low cost, and high theoretical energy density. Herein, a flexible porous bifunctional electrode with both electrocatalytic and photocatalytic activity was synthesized and introduced as a cathode to assemble a high-performance Li–O₂ battery that achieved an overpotential of 0.19 V by charging with the aid of solar energy. As a proof-of-concept application, a flexible Li–O₂ battery was constructed and integrated with a solar cell via a scalable encapsulate method to fabricate a flexible self-powered energy system with excellent flexibility and mechanical stability. Moreover, by exploring the evolution of the electrode morphology and discharge products (Li₂O₂), the charging process of the Li–O₂ battery powered by solar energy and solar cell was demonstrated.

With the increasing demand for wearable electronics and portable devices for applications in communication, environmental monitoring, and personal health care, the development of flexible, portable, and environmentally friendly sustainable energy supply and energy storage systems is of great significance for the realization of the next-generation intelligent society and the improvement of our quality of life.^[1–5] Self-powered nanotechnology has been proposed as a promising technology for powering flexible and wearable electronics to operate independently and sustainably by combining an energy supply system that can harvest energy

from the environment and an energy storage device possessing extended lifespan.^[6,7]

Today's energy supply strongly depends on fossil fuels with limited minable years, such as oil, coal, and natural gas. These energy sources usually lead to serious environmental problems and are not portable, which severely restrict their application in the field of mobile electronics. Developing a renewable and environmentally friendly portable energy supply system that can be collected and stored in the surrounding environment, such as wind, solar, thermal, and mechanical energy, and so forth has become an important issue. Among the above energy sources, solar power generation may be the most attractive that is mature and portable.^[8,9] More recently, profit from the development of more efficient and less expensive flexible solar cells, solar energy has triggered wide interest and has been used as a promising energy supply system for portable electronics and wearable devices owing to its abundant supply, low cost, sustainability, and easy harvest.^[10,11] However, with the diurnal cycle and the fluctuation of sunlight intensity, the output of solar cells are intermittent and unstable.^[12,13] In this context, appropriate energy storage devices are quite necessary to offset the fluctuations of solar power and to construct a reliable and durable self-powered energy system.

To date, many attempts have been devoted to developing a series of self-powered energy supply systems by integrating solar cells with supercapacitors or Li-ion batteries.^[14–16] However, the relatively low energy density of existing energy storage devices still limits their wide application in the self-powered system.^[17,18] Recently, the lithium–oxygen (Li–O₂) battery has emerged as a competitive system with an extremely high theoretical energy density of 3500 Wh kg^{–1}, which holds great promise to construct a self-powered system by combining with solar cells.^[19–23] Unfortunately, a high overpotential and poor cycle life of the Li–O₂ battery remain critical challenges to overcome.^[24] Therefore, it is necessary to develop an efficient cathode with high electrocatalytic activity and electrochemical stability to simultaneously meet these essential challenges. According to previous research, the introduction of a photocatalyst can notably reduce the overpotential of the Li–O₂ battery and solar energy can be employed to compensate the electric energy during the charging process.^[25,26] As the charging process is powered by the solar cell in the self-powered energy system, the integration of solar energy into the Li–O₂ battery during the charging process to further decrease the serious polarization. In this regard, explore an appropriate bifunctional Li–O₂ battery electrode with both electrocatalytic and photocatalytic activity is highly desired.

[*] X.–y. Yang, Prof. Dr. J.–m. Yan

Key Laboratory of Automobile Materials (Jilin University), Ministry of Education, Department of Materials Science and Engineering
Jilin University, Changchun, 130022 (P. R. China)
E-mail: junminyan@jlu.edu.cn


X.–y. Yang, Prof. Dr. X.–b. Zhang

State Key Laboratory of Rare Earth Resource Utilization, Changchun Institute of Applied Chemistry, Chinese Academy of Sciences
Changchun, 130022 (P. R. China)
E-mail: xbzhang@ciac.ac.cn

X.–l. Feng, X. Jin, M.–z. Shao, B.–l. Yan, Prof. Dr. Y. Zhang
Key Laboratory of Bio-inspired Smart Interfacial Science and Technology of Ministry of Education, School of Chemistry
Beihang University, Beijing 100191 (P. R. China)
E-mail: jade@buaa.edu.cn

Prof. Dr. Y. Zhang

Beijing Advanced Innovation Center for Biomedical Engineering
Beihang University, Beijing 100191 (P. R. China)

 Supporting information and the ORCID identification number(s) for the author(s) of this article can be found under:
<https://doi.org/10.1002/anie.201907805>.

In our work, porous TiN/TiO₂ composite nanowires (NWs) are grown in situ on carbon cloth (TT@CC) to construct a bifunctional flexible Li-O₂ battery cathode by a facile hydrothermal method and thermal treatment under relative low temperature. The Li-O₂ batteries with a TT@CC cathode exhibit excellent performance, including higher specific capacity, lower overpotential, and long cycle life. Moreover, thanks to the photocatalytic activity of the TT@CC cathode, the overpotential of the battery can be further decreased to 0.19 V with the aid of solar energy during the charging process. Subsequently, we designed a flexible Li-O₂ battery based on the TT@CC cathode and present a convenient encapsulation method to combine the as-fabricated flexible Li-O₂ battery with a commercial solar cell to construct a flexible self-powered energy system. Importantly, the as-fabricated self-powered energy system can light a red light-emitting diode (LED) constantly with or without illumination, showing its potential application in flexible and wearable electronic devices. By exploring the evolution of the electrode morphology and discharge product Li₂O₂, we have demonstrated the charging process of the Li-O₂ battery powered by solar energy and solar cell.

As shown in Figure 1 a, the TT@CC cathode was obtained by a two-step processes. Firstly, via a self-assembly hydrothermal method, the TiO₂ NWs were grown on the carbon cloth densely and homogeneously. After the melamine coordination thermal treatment process, the TT@CC cathodes were obtained. The color of electrode changed from black to white then to black after each step (Supporting Information, Figure S1). Scanning electron microscopy (SEM) was used to characterize the morphology and structure evolution. After the hydrothermal process, the smooth surface of the carbon cloth fiber (Figure 1 b) was covered uniformly with TiO₂ NWs, the diameters of which were in a typical range between 50 and 100 nm and lengths were about 1 μ m (Figure 1 c). As shown in Figure 1 d, the pristine structure of the TiO₂ NWs was

maintained after thermal treatment azotizing reaction. The orderly structure can provide sufficient space to store the discharge products. The phase and surface elemental analysis of the obtained electrode were then investigated by X-ray diffraction (XRD) and X-ray photoelectron spectroscopy (XPS). As illustrated in Figure 1 e, all peaks of the electrode can match well with the pure TiN phase with a cubic structure at 36.7°, 42.6°, and 61.8°.^[27] The high-resolution Ti 2p XPS spectrum presented in Figure 1 f clearly shows that the presence of TiN and TiO₂.^[28,29] The nitrogen presented on the electrode after the thermal treatment process (Supporting Information, Figures S2 and S3).^[29,30] Interestingly, the transmission electron microscopy (TEM) images reveal that the obtained TiN/TiO₂ NW is fabricated with a large number of nanoparticles, which construct a porous structure (Supporting Information, Figure S4). The nitrogen adsorption/desorption isotherm illustrates the mesoporous features of the obtained electrode, with a Brunauer–Emmett–Teller (BET) surface area of 96.3 m² g⁻¹ (Supporting Information, Figure S5). Thanks to the orderly networks and highly porous structure, the obtained TT@CC cathode can ensure the transport of both electrons and gas around the cathode efficiently during the discharge–charge processes.^[31] The high-magnification transmission electron microscopy (HRTEM) image (Supporting Information, Figure S6) shows the lattice interlayer spacing of 0.21 nm and 0.25 nm, which is nearly consistent with the (200) and (111) lattice plane of cubic TiN.^[28] Moreover, energy-dispersive X-ray spectroscopy (EDS) element mapping confirm that the Ti, N, and O elements, which belong to TiN/TiO₂ NWs, distribute on the carbon cloth fiber surface homogeneously (Supporting Information, Figure S7). The bright contrast in the high-angle annular dark-field (HAADF) STEM image of a single porous TiN/TiO₂ NW and corresponding EDS mappings (Figure 1 g) also show clearly that the occupancies of Ti, N, and O elements distribute uniformly along the nanowire. All these results indicate the successful synthesis of TT@CC bifunctional electrode.

Thanks to the unique orderly porous structure and the high electrocatalytic activity of the TT@CC cathode, as a proof-of-concept application, the TT@CC was utilized as a free-standing Li-O₂ battery cathode directly. For comparison, pristine carbon cloth (Pristine-CC) and TiO₂@CC cathode were also tested. Among the first discharge–charge cycle, the overpotential of the Li-O₂ battery with TT@CC cathode is only 0.88 V, which is much lower than that with Pristine-CC (1.64 V) and TiO₂@CC (1.29 V) (Figure 2 a), indicating that the TT@CC cathode exhibits superior electrocatalytic activity over the comparison cathode. This result is further demonstrated by cyclic voltammetry (CV) at a scan rate of 0.1 mV s⁻¹ (Supporting Information, Figure S8).^[19] Notably, the TT@CC cathode can deliver an extremely high capacity (9622 mAh g⁻¹) at a discharge current density of 100 mA h g⁻¹ and still have 2032 mAh g⁻¹ even at a current density of 2 Ag⁻¹ (Figure 2 b). The discharge capacity of TiO₂@CC cathode and TT@CC cathode under argon (Ar) atmosphere were also tested to confirm that the background capacity is ignorable under the voltage range (Supporting Information, Figure S9). Unexpectedly, even after the first deep discharge process, the TT@CC cathode still keep

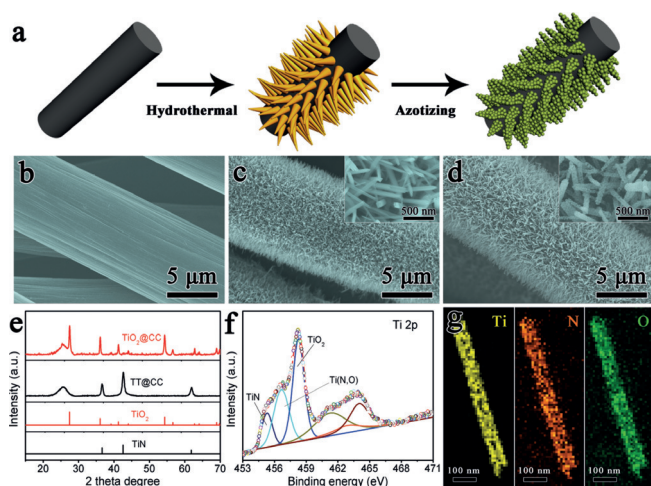


Figure 1. a) Representations of the design and preparation of the TT@CC cathode; b)–d) SEM images of the pristine-CC, TiO₂@CC, and TT@CC (insets are enlarged SEM images); e) XRD patterns of the TiO₂@CC and TT@CC; f) High-resolution Ti 2p XPS spectra of the resultant TT@CC cathode; and g) STEM EDS element mapping of Ti, N, and O of a single TiN/TiO₂ NW.

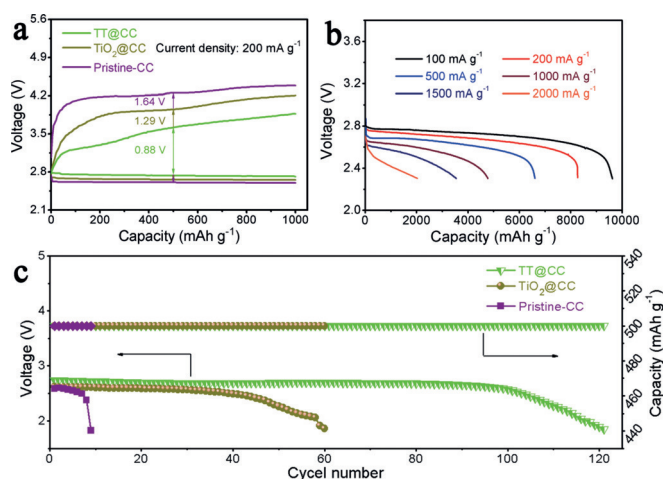


Figure 2. a) The first discharge–charge curves of the Li–O₂ batteries with three different cathodes; b) discharge curves of the Li–O₂ battery with the TT@CC cathode at different current densities with the voltage restricted to 2.3 V; c) the terminal discharge voltage of the Li–O₂ batteries with three different cathodes at a current density of 250 mA g^{−1}.

a 100% coulombic efficiency between 2.3–4.0 V, indicating the high reversibility of the TT@CC cathode (Supporting Information, Figure S10). The following rate performance comparison reveals that the Li–O₂ battery with TT@CC cathode has a much higher discharge voltage plateau than that with Pristine-CC and TiO₂@CC at a wide variety of current densities (Supporting Information, Figure S11). The cycling performance of the Li–O₂ batteries were tested by galvanostatic cycling at a current density of 250 mA g^{−1} with a capacity of 500 mAh g^{−1}. Obviously, the terminal discharge voltage of the Li–O₂ battery with the TT@CC cathode can still maintain above 2.0 V even after 120 cycles. In contrast, the terminal discharge voltages of the battery with Pristine-CC and TiO₂@CC cathode decreased to <2.0 V after only 8 and 60 cycles, respectively (Figure 2c).

To investigate the photocatalytic activity of TT@CC cathode and the performance of Li–O₂ battery with TT@CC cathode powered by solar energy, we fabricate a Li–O₂ battery with special design battery case to ensure that the TT@CC cathode can absorb solar energy as full as possible. The charge–discharge performance of the batteries was tested under the same conditions, except with and without illumination, to provide an objective comparison. Without illumination, the Li–O₂ battery shows a charge midpoint voltage of 3.65 V, which is similar to the previous test. In sharp contrast, a lower charge midpoint voltage of 2.94 V can be achieved upon charging under illumination (Figure 3a). It may be because the electron–hole pair will generate on the surface of excited TT@CC cathode under illumination. Subsequently, under the driving force between valance band (VB) potential of TT@CC and O₂/Li₂O₂ redox potential, the photoexcited electron holes in the VB will oxidize the Li₂O₂ and then compensate the electric energy during the charging process.^[32] With the aid of solar energy, the Li–O₂ battery can achieve an energy-conversion efficiency of about 94% with the overpotential of 0.19 V. Figure 3b reveals the dynamic light-

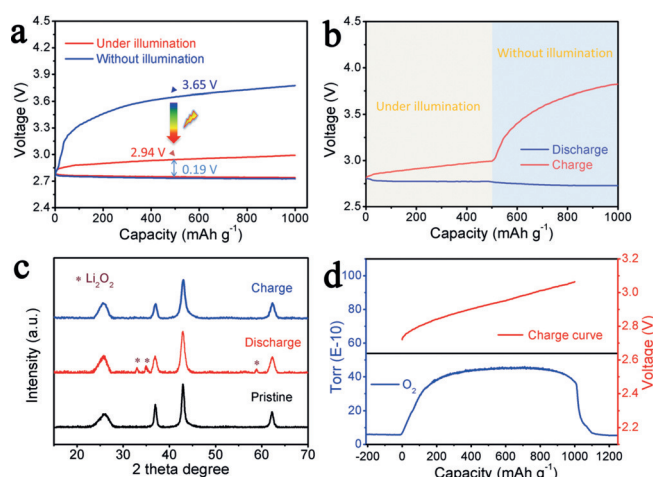


Figure 3. a) The discharge–charge curves of the Li–O₂ batteries with or without illumination; b) dynamic light-response discharge–charge voltage of the Li–O₂ battery; c) XRD pattern of the pristine, discharged, and solar-energy-aided charged TT@CC cathode; d) DEMS curve of the Li–O₂ battery charge with the aid of solar energy.

response discharge–charge voltage of the Li–O₂ battery when illumination was switched from on to off. Once illumination was removed, the charge voltage increased immediately. Such light-response behavior further supports our proposed purpose that solar energy can be used to compensate the electric energy during the charging process to further reduce the serious polarization of Li–O₂ battery.

To better demonstrate the charging process powered by solar energy, we carried out XRD and SEM to detect the discharge product before and after the charging process. Three characteristic diffraction peaks of Li₂O₂ are observed in the XRD pattern of the TT@CC cathode after the discharging process, which reveals that the discharge product is Li₂O₂.^[17,18] The Li₂O₂ can be decomposed completely after subsequent solar-energy-aided charging progress (Figure 3c). The SEM images also demonstrate that Li₂O₂ particles are completely decomposed after the charging process, in accordance with the XRD data (Supporting Information, Figure S12). We further confirmed the decomposition process of Li₂O₂ by using in situ differential electrochemical mass spectrometry (DEMS) analysis. As shown in Figure 3d, the relative pressure of oxygen is increased continuously along with the charging process until a stable value, which means the decomposition of Li₂O₂ to produce O₂ during the charging process. All of the above results suggest that the charging process of Li–O₂ battery powered by solar energy is via decomposition of Li₂O₂ under an extremely low overpotential.^[33]

As a proof-of-concept experiment, inspired by the requirement of flexible energy devices for wearable and portable electronics in the last few years, we fabricated a flexible integrated self-powered energy system via a simple encapsulation method. Figure 4a illustrates the self-powered energy system. Figure 4b,c illustrates the different operation conditions and mechanism of the as-fabricated solar cell/Li–O₂ battery hybrid self-powered energy system. Under illumination, the solar cell operated as the energy supply to power

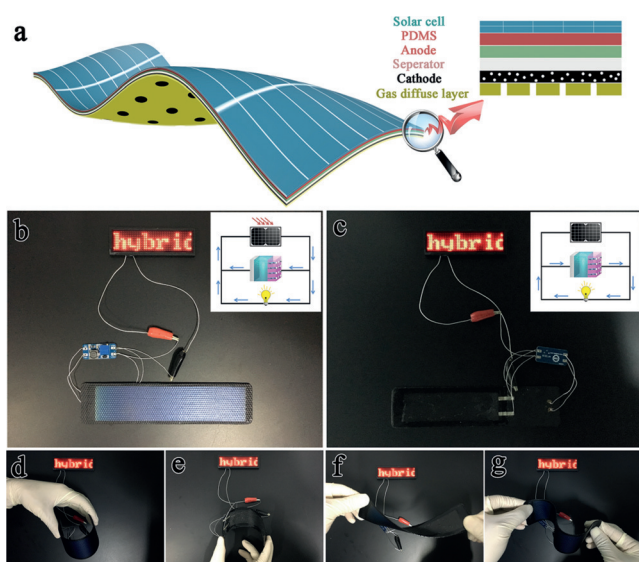


Figure 4. a) Illustration of the structure of the self-powered energy system; b),c) digital photograph of the assembled self-powered energy system working with or without the light; inset shows the working circuit connection; d)–g) the self-powered energy system powering a commercial red LED display screen at various bent and twisted conditions.

the LED and charge the Li-O₂ battery. After the illumination was removed, the stored energy in the Li-O₂ battery switched as the energy supply for the LED, which maintained this system working continuously for a very long time. The insets clearly illustrate the working circuit under different operating conditions. To further explore the flexibility of the self-powered energy system, the as-fabricated device was bent and twisted into different shapes. Surprisingly, the LED was bright constantly under various testing conditions (Figure 4d–g), indicating the excellent flexibility and mechanical stability of the as-fabricated self-powered energy system. The discharge curves of the flexible Li-O₂ batteries under different bending conditions also show the electrochemical and mechanical stability of the battery under various deformation conditions (Supporting Information, Figure S13). The decomposition processes of Li₂O₂ were also explored by SEM, XRD, and Fourier transform IR spectroscopy (FTIR) to demonstrate the rechargeability of the flexible Li-O₂ battery with the TT@CC cathode integrated into the self-powered energy system charged by the solar cell (Supporting Information, Figures S14–S16).

In conclusion, a porous self-standing bifunctional flexible TT@CC cathode was successfully designed and synthesized by a facile hydrothermal method and thermal treatment under relative low temperature. Thanks to the unique structure and electrocatalytic activity of the TT@CC cathode, the Li-O₂ batteries with TT@CC cathode can deliver excellent electrochemical performance, including high specific capacity, superior rate capability, and long cycle life. Amazingly, the overpotential of the Li-O₂ battery with the TT@CC cathode can be further decreased to 0.19 V and achieve an energy conversion efficiency of about 94% by charging with the aid of solar energy. As a proof-of-concept application, we

constructed a flexible integrated self-powered energy system by a convenient encapsulation method. Such a self-powered energy system could constantly power a commercial LED even under all the test deformation conditions, demonstrating excellent flexibility and showing great potential for future applications in powering flexible and wearable electronics. Moreover, by exploring the decomposition processes of the Li₂O₂, we demonstrate the rechargeability of the Li-O₂ battery with the TT@CC cathode powered by solar energy and solar cell. Although the solar cell/Li-O₂ battery flexible hybrid energy conversion and storage device provides a new strategy to construct the self-powered energy system, advanced control circuitry needs to be developed and integrated to control the operating state of the system precisely.

Acknowledgements

This work was financially supported by National Natural Science Foundation of China (Grant Nos. 21725103 and 21771013). National Key R&D Program of China (2016YFB0100100).

Conflict of interest

The authors declare no conflict of interest.

Keywords: bifunctional electrodes · flexible batteries · Li-O₂ batteries · solar energy conversion

How to cite: *Angew. Chem. Int. Ed.* **2019**, *58*, 16411–16415
Angew. Chem. **2019**, *131*, 16563–16567

- [1] L. Wang, D. Chen, K. Jiang, G. Shen, *Chem. Soc. Rev.* **2017**, *46*, 6764–6815.
- [2] W. Gao, S. Emaminejad, H. Y. Nyein, S. Challa, K. Chen, A. Peck, H. M. Fahad, H. Ota, H. Shiraki, D. Kiriya, D. H. Lien, G. A. Brooks, R. W. Davis, A. Javey, *Nature* **2016**, *529*, 509–514.
- [3] X. Wang, Z. Liu, T. Zhang, *Small* **2017**, *13*, 1602790.
- [4] L. Li, Z. Wu, S. Yuan, X.-B. Zhang, *Energy Environ. Sci.* **2014**, *7*, 2101–2122.
- [5] K. Xie, B. Wei, *Adv. Mater.* **2014**, *26*, 3592–3617.
- [6] X. Xiao, T. Li, P. Yang, Y. Gao, H. Jin, W. Ni, W. Zhan, X. Zhang, Y. Cao, J. Zhong, L. Gong, W. C. Yen, W. Mai, J. Chen, K. Huo, Y. L. Chueh, Z. L. Wang, J. Zhou, *ACS Nano* **2012**, *6*, 9200–9206.
- [7] S. Xu, Y. Qin, C. Xu, Y. Wei, R. Yang, Z. L. Wang, *Nat. Nanotechnol.* **2010**, *5*, 366–373.
- [8] N. S. Lewis, *Science* **2007**, *315*, 798–801.
- [9] N. S. Lewis, *Chem. Rev.* **2015**, *115*, 12631–12632.
- [10] P. Docampo, J. M. Ball, M. Darwich, G. E. Eperon, H. J. Snaith, *Nat. Commun.* **2013**, *4*, 2761.
- [11] J. Y. Kim, S. H. Kim, H. H. Lee, K. Lee, W. Ma, X. Gong, A. J. Heeger, *Adv. Mater.* **2006**, *18*, 572–576.
- [12] A. Mellit, A. Massi Pavan, V. Lughì, *Sol. Energy* **2014**, *105*, 401–413.
- [13] K. S. Tey, S. Mekhilef, *Sol. Energy* **2014**, *101*, 333–342.
- [14] X. Xu, S. Li, H. Zhang, Y. Shen, S. M. Zakeeruddin, M. Graetzel, Y. B. Cheng, M. Wang, *ACS Nano* **2015**, *9*, 1782–1787.

- [15] Z. L. Wang, J. Chen, L. Lin, *Energy Environ. Sci.* **2015**, *8*, 2250–2282.
- [16] P. Yang, X. Xiao, Y. Li, Y. Ding, P. Qiang, X. Tan, W. Mai, Z. Lin, W. Wu, T. Li, H. Jin, P. Liu, J. Zhou, C. P. Wong, Z. L. Wang, *ACS Nano* **2013**, *7*, 2617–2626.
- [17] X.-y. Yang, J.-j. Xu, D. Bao, Z.-w. Chang, D.-p. Liu, Y. Zhang, X.-B. Zhang, *Adv. Mater.* **2017**, *29*, 1700378.
- [18] T. Liu, J. J. Xu, Q. C. Liu, Z. W. Chang, Y. B. Yin, X. Y. Yang, X. B. Zhang, *Small* **2017**, *13*, 1602952.
- [19] J.-J. Xu, Z.-W. Chang, Y.-B. Yin, X.-B. Zhang, *ACS Cent. Sci.* **2017**, *3*, 598–604.
- [20] L. Johnson, C. Li, Z. Liu, Y. Chen, S. A. Freunberger, P. C. Ashok, B. B. Praveen, K. Dholakia, J. M. Tarascon, P. G. Bruce, *Nat. Chem.* **2014**, *6*, 1091–1099.
- [21] J. J. Xu, Z. L. Wang, D. Xu, L. L. Zhang, X. B. Zhang, *Nat. Commun.* **2013**, *4*, 2438.
- [22] R. Black, B. Adams, L. Nazar, *Adv. Energy Mater.* **2012**, *2*, 801–815.
- [23] T. Liu, M. Leskes, W. Yu, A. J. Moore, L. Zhou, P. M. Bayley, G. Kim, C. P. Grey, *Science* **2015**, *350*, 530–533.
- [24] Z.-W. Chang, J.-J. Xu, X.-B. Zhang, *Adv. Energy Mater.* **2017**, *7*, 1700875.
- [25] M. Yu, X. Ren, L. Ma, Y. Wu, *Nat. Commun.* **2014**, *5*, 5111.
- [26] Y. Liu, N. Li, S. Wu, K. Liao, K. Zhu, J. Yi, H. Zhou, *Energy Environ. Sci.* **2015**, *8*, 2664–2667.
- [27] J. Park, Y.-S. Jun, W.-r. Lee, J. A. Gerbec, K. A. See, G. D. Stucky, *Chem. Mater.* **2013**, *25*, 3779–3781.
- [28] X. Lu, G. Wang, T. Zhai, M. Yu, S. Xie, Y. Ling, C. Liang, Y. Tong, Y. Li, *Nano Lett.* **2012**, *12*, 5376–5381.
- [29] I. Miloš, H.-H. Strehblow, B. Navinšek, M. Metikoš-Huković, *Surf Interface Anal.* **1995**, *23*, 529–539.
- [30] Y. Chang, S. Dong, Y. Ju, D. Xiao, X. Zhou, L. Zhang, X. Chen, C. Shang, L. Gu, Z. Peng, G. Cui, *Adv. Sci.* **2015**, *2*, 1500092.
- [31] Y. B. Yin, J. J. Xu, Q. C. Liu, X. B. Zhang, *Adv. Mater.* **2016**, *28*, 7494–7500.
- [32] Y. Liu, J. Yia, Y. Qiao, D. Wang, P. He, Q. Li, S. Wu, H. Zhou, *Energy Storage Mater.* **2018**, *11*, 170–175.
- [33] B. Zhou, L. Guo, Y. Zhang, J. Wang, L. Ma, W.-H. Zhang, Z. Fu, Z. Peng, *Adv. Mater.* **2017**, *29*, 1701568.

Manuscript received: June 23, 2019

Revised manuscript received: August 4, 2019

Accepted manuscript online: September 5, 2019

Version of record online: October 4, 2019